DISTRIBUTED BEAMFORMING FOR WIRELESS SENSOR NETWORKS WITH RANDOM NODE LOCATION

Keyvan Zarifi, Sofiene Affes

INRS-EMT, Université du Québec,
Montréal, QC, H5A 1K6, Canada

Ali Ghrayeb

Concordia University
Montreal, QC, H3G 1M8, Canada

ABSTRACT

Due to the unsupervised nature of wireless sensor networks (WSNs), intensive communications are required among the selected nodes to reach a consensus and synchronize prior to entering a distributed beamforming (DBF) procedure. Therefore, a sensible approach to select the nodes should not only take into account the required beampattern, but also should aim to preserve the inter-node connectivity and the network energy. We show for a uniformly distributed WSN that when the nodes are selected from a ring of proper radii, the resulting beampattern mainlobe is narrower compared to that of the classical DBF technique proposed in [1]. At the same time, our proposed technique may preserve a substantial amount of network energy and reduce the probability of network disconnectivity. Directivity of the proposed DBF technique is analyzed and an extension of the technique to a multi-ring case is presented. It is shown that the sidelobe peaks can be considerably decreased if the nodes are selected from multiple concentric rings.

Index Terms— Beampattern, Distributed beamforming, Network energy consumption, Wireless sensor networks.

1. INTRODUCTION

One of the challenging problems in wireless sensor networks (WSNs) is establishing a reliable and energy-efficient communication link between small battery-powered sensor nodes that have a limited transmission range and an access point that is typically located far away from the network. To tackle this problem, the distributed beamforming (DBF) technique has recently been introduced [1]-[3] using which selected nodes from a network cluster transmit their common message with proper weights such that their transmitted signals are coherently combined in the direction of the intended access point. As a result, the nodes collective transmission range is substantially increased without requiring to amplify their total transmission power.

In many DBF applications, the beampattern mainlobe should be narrow enough to concentrate most of the transmitted power towards the intended access point while inflicting low interference on unintended receivers such as other clusters' access points. When the nodes are uniformly distributed on a plane, the mainlobe width of the average beampattern is approximately inverse proportional to the radius of the disk from which the nodes are selected to participate in the DBF [1]. This may cause a substantial problem if the desired mainlobe width necessitates selecting the nodes from a disk larger than the cluster area. Note also that the nodes participating

in the DBF are independent units and their common message should first be distributed, or, generated as a consensus [4] among all nodes.[1] In addition, all the selected nodes should be synchronized to be able to act as a virtual antenna array. The above facts necessitate quite intensive inter-node communication prior to the actual DBF. However, given the fix number of participating nodes in the DBF, larger disk radius equals larger average distances between the selected nodes. This, in turn, results in an increased probability of disconnectivity among the selected nodes.

In this paper, we show that when the nodes are selected from a ring of proper radii, the mainlobe of the average beampattern narrows down, and, moreover, significant amount of network energy may be preserved and the probability of network disconnectivity can be considerably reduced. We analyze the average beampattern for such a node selection approach and derive sidelobe nulls and peaks and a lower bound on the directivity of the proposed DBF. Selecting the nodes from multiple concentric rings, we further show how the sidelobe peaks levels can be substantially reduced.

The rest of the paper is organized as follows. Section 2 represents the proposed DBF technique and Section 3 analyzes its average beampattern properties. Section 4 extends the proposed technique to the multi-ring scenario and Section 5 concludes the paper.

2. THE PROPOSED TECHNIQUE

Consider a large wireless sensor network whose nodes are uniformly distributed on a two-dimensional plane and an access point located in the far field of the same plane. Let $S(O, R_i, R_o)$ denote the ring centered at a point O with the inner radius $R_i \geq 0$ and the outer radius $R_o > R_i$ in a network cluster. The ring has an area $A_S = \pi(R_o^2 - R_i^2)$ that is large enough to include N nodes. These nodes communicate with one another to reach a consensus [4]. Then $K \leq N$ nodes are randomly selected, and, following a distributed synchronization procedure [2], [5], jointly transmit their common narrow-band message with the primary aim to maximize the received power at the direction of their access point. Note that, N should be large enough such that the consensus reached by the participating nodes is an accurate approximation of the consensus of the whole network cluster, and $K \leq N$ should be just large enough to keep the SNR at the access point above a certain threshold. Further increasing

---

[1]The consensus can be any quantity of interest such as the average of the sensed (received) signals at nodes.

K may contribute to nodes unnecessary power depletion.[2]

Without any loss of generality, we choose O as the pole and the axis connecting O to the access point as the x-axis of a polar coordinate system. Let (r_k, ψ_k) and $(P, \phi_0 = 0)$ denote the polar coordinates of the node k and the access point, respectively. Given the location vectors of the selected nodes $\mathbf{r} = [r_1, r_2, \ldots, r_K]$ and $\boldsymbol{\psi} = [\psi_1, \psi_2, \ldots, \psi_K]$, the corresponding array factor at a point (P, ϕ) can be written as

$$F(\phi, \mathbf{r}, \boldsymbol{\psi}) = \frac{1}{K} \sum_{k=1}^{K} e^{j\xi_k} e^{j\frac{2\pi}{\lambda} d_k(\phi)} \tag{1}$$

where ξ_k is the initial phase of node k, λ is the carrier wavelength, and $d_k(\phi) = \left(P^2 + r_k^2 - 2Pr_k \cos(\phi - \psi_k)\right)^{1/2}$ is the Euclidian distance between the k-th node and (P, ϕ). The received signal at the access point is maximized when $\xi_k = -2\pi d_k(0)/\lambda$ [1], [3]. Moreover, as the access point is in the far-field, we have that $d_k(\phi) \approx P - r_k \cos(\phi - \psi_k)$. Using the latter results in (1), it follows that the array factor is approximately given by [1], [3]

$$\tilde{F}(\phi, \mathbf{r}, \boldsymbol{\psi}) = \frac{1}{K} \sum_{k=1}^{K} e^{j\frac{2\pi}{\lambda} r_k (\cos(\psi_k) - \cos(\phi - \psi_k))} = \frac{1}{K} \sum_{k=1}^{K} e^{-\beta(\phi) z_k} \tag{2}$$

where $\beta(\phi) \triangleq \frac{4\pi}{\lambda} \sin\left(\frac{\phi}{2}\right)$ and $z_k \triangleq r_k \sin \tilde{\psi}_k$ with $\tilde{\psi}_k \triangleq \psi_k - \frac{\phi}{2}$. Note that, as the selected nodes are uniformly distributed on $S(O, R_i, R_o)$, r_k and $\tilde{\psi}_k$ are the realizations of random variables R and Ψ, respectively, where

$$f_R(r_k) = \begin{cases} 2r_k A_S^{-1} & R_i \leq r_k \leq R_o \\ 0 & \text{else} \end{cases}, \quad f_\Psi(\tilde{\psi}_k) = \frac{1}{2\pi}. \quad -\pi \leq \tilde{\psi} < \pi \tag{3}$$

For the random variables R and Ψ as defined in (3), it can be shown that the probability density function of $Z \triangleq R \sin \Psi$ is given by [6]

$$f_Z(z) = \begin{cases} 2A_S^{-1}(g(z, R_o) - g(z, R_i)) & 0 \leq |z| < R_i \\ 2A_S^{-1} g(z, R_o) & R_i \leq |z| \leq R_o \end{cases} \tag{4}$$

where $g(z, t) = t\sqrt{1 - (z/t)^2}$. It follows from the above discussion that Equation (2) can be alternatively represented as $\tilde{F}(\phi, \mathbf{z}) = \frac{1}{K} \sum_{k=1}^{K} e^{-j\beta(\phi) z_k}$ where $\mathbf{z} \triangleq [z_1, z_2, \ldots, z_K]$ is a realization of a random vector $\mathbb{Z} = [Z_1, Z_2, \ldots, Z_K]$ with independent entries all of which are identically distributed according to (4). The far-field beampattern associated with the array factor $\tilde{F}(\phi, \mathbf{z})$ is given by $P(\phi, \mathbf{z}) = |\tilde{F}(\phi, \mathbf{z})|^2$. As $P(\phi, \mathbf{z})$ depends on the realizations of $\mathbb{Z}$, the study of the behavior of $P_{\text{av}}(\phi) \triangleq E_{\mathbb{Z}}\{P(\phi, \mathbb{Z})\}$ is of prominent importance. Note also that since the entries of $\mathbb{Z}$ are independently distributed, it can be readily shown that for any arbitrary realization $\mathbf{z}$ of $\mathbb{Z}$, we have that $\lim_{K \to \infty} P(\phi, \mathbf{z}) = P_{\text{av}}$ (see also [1] for a similar observation). This further motivates the analysis of $P_{\text{av}}(\phi)$.

3. AVERAGE BEAMPATTERN ANALYSIS

It is proven in [6] that if a random variable Z is distributed as in (4), then

$$E\left\{e^{j\beta(\phi)Z}\right\} = \frac{2}{R_o^2 - R_i^2} \left(\frac{R_o}{\beta(\phi)} J_1(R_o\beta(\phi)) - \frac{R_i}{\beta(\phi)} J_1(R_i\beta(\phi))\right) \tag{5}$$

where $J_n(\cdot)$ is the n-th order Bessel function of the first kind. Using (5) along with the fact that the entries of $\mathbb{Z}$ are independently distributed, it can be readily shown that [6]

$$P_{\text{av}}(\phi) = \frac{1}{K} + \left(1 - \frac{1}{K}\right) \left|E\left\{e^{j\beta(\phi)Z}\right\}\right|^2. \tag{6}$$

Note that when $R_i = 0$, that is, when the ring $S(O, R_i, R_o)$ reduces to $D(O, R_o)$, a disc centered at O with radius R_o, it can be directly shown from (6) that $P_{\text{av}}(\phi) = 1/K + (1 - 1/K) |2J_1(R_o\beta(\phi))/R_o\beta(\phi)|^2$. The same expression has been obtained for $P_{\text{av}}(\phi)$ in [1] that exclusively investigates the special case of $R_i = 0$. In what follows, we explore the properties of $P_{\text{av}}(\phi)$ in (6) in more details and explain some advantages of choosing $R_i \neq 0$ with respect to the conventional approach of [1] that proposes to select the nodes from $D(O, R_o)$.

3.1. The mainlobe of the beampattern: It is crucial to form a beampattern with narrow mainlobe in many practical scenarios. In our context, such a requirement may be translated into having $\phi_{(n),1}$, the first null of $E\{e^{j\beta(\phi)Z}\}$ in (5), or, equivalently, the first minimum point of $P_{\text{av}}(\phi)$ in (6), close to $\phi_0 = 0$. It can be proven that, for a given R_o, $\phi_{(n),1}$ is a decreasing function of R_i. To show this, let $\alpha = R_i/R_o$. From (5) we have $E\{e^{j\beta(\phi)Z}\} = f(R_o\beta(\phi), \alpha)$ where

$$f(x, \alpha) = \frac{2}{1 - \alpha^2} \left(\frac{J_1(x)}{x} - \frac{\alpha J_1(\alpha x)}{x}\right). \qquad 0 \leq \alpha < 1 \tag{7}$$

The following theorem holds [6].

Theorem 1: Let $x^*(\alpha)$ denote the smallest positive number such that $f(x^*(\alpha), \alpha) = 0$. We have $x^*(0) = \nu_1$ and $\lim_{\alpha \to 1^-} x^*(\alpha) = \nu_0$, where $\nu_1 \approx 3.8317$ and $\nu_0 \approx 2.4048$ are the first positive roots of $J_1(x)$ and $J_0(x)$, respectively. For any $\alpha \in (0, 1)$, we have that $\nu_0 < x^*(\alpha) < \nu_1$. Moreover, $x^*(\alpha)$ is the only root of $f(x, \alpha)$ in the interval (ν_0, ν_1), and $dx^*(\alpha)/d\alpha < 0$.

Theorem 1 shows that, if $R_i = 0$, then, $R_o\beta(\phi_{(n),1}) = \nu_1$, or, equivalently, $\phi_{(n),1} = 2\arcsin\left((4\pi R_o)^{-1}\lambda\nu_1\right)$. Meanwhile, increasing R_i continuously decreases $\phi_{(n),1}$, such that when $R_i \approx R_o$, we have $\phi_{(n),1} \approx 2\arcsin\left((4\pi R_o)^{-1}\lambda\nu_0\right)$. Note that, as R_o is usually large, R_i can be a very close to R_o without causing the nodes on $S(O, R_i, R_o)$ drop below N. Moreover, for a large R_o/λ, we have that $\phi_{(n),1} \approx (2\pi R_o)^{-1}\lambda\nu_1$ for $R_i = 0$ and $\phi_{(n),1} \approx (2\pi R_o)^{-1}\lambda\nu_0$ for $R_i \approx R_o$. This simply means that, for a given R_o, the first minimum point of the average beampattern can be reduced up to 37% by increasing R_i from zero to R_o. Similarly, for a given target $\phi_{(n),1}$, the outer radius of the ring S can be decreased from $R_o \approx (2\pi\phi_{(n),1})^{-1}\lambda\nu_1$ to $R_o \approx (2\pi\phi_{(n),1})^{-1}\lambda\nu_0$, just by increasing R_i from zero to $R_i \approx R_o \approx (2\pi\phi_{(n),1})^{-1}\lambda\nu_0$. This property can be very useful when the cluster nodes are confined to an area that is smaller than a disk of radius $(2\pi\phi_{(n),1})^{-1}\lambda\nu_1$.

3.2. The network energy: In the DBF scheme presented above, the nodes on $D(O, R_i)$ as well as the unselected nodes from $S(O, R_i, R_o)$ are used neither in generating the consensus nor in the DBF, and, therefore, may be left in the sleeping mode. Note that, a node using a typical transceiver with the transmission range of several tens of meters has a power consumption in the range of 10-20 mW in the transmission/listening mode while its power consumption in the

sleeping mode is in the range of 10 μW [7]. It should also be mentioned that, the number of inter-node transmissions required to reach a certain vicinity of the consensus at least linearly increases with the number of nodes participating in the consensus reaching process [4]. Therefore, even if one extra node, say, from $D(O, R_i)$, decides to participate in this process, the total number of required inter-node transmissions may considerably increase. Therefore, the technique proposed here tends to save a substantial amount of energy as compared to the techniques that use all available nodes on $D(O, R_o)$.

Instead of selecting the nodes from $S(O, R_i, R_o)$, it is also possible to randomly choose them from $D(O, R_o)$ and make the selected nodes reach a consensus, while leaving all other nodes in the sleeping mode. After the N selected nodes reached a consensus, K nodes are randomly selected from them and perform the DBF. Although such an approach increases $\phi_{(n),1}$ to its maximum value of $2 \arcsin \left((4\pi R_o)^{-1} \lambda \nu_1\right)$, one may argue that, as long as the energy preserving is concerned, it is immaterial whether the N active nodes are selected from $D(O, R_o)$ or from $S(O, R_i, R_o)$. As will be shown below, this may not be a correct argument. The nodes have to intensively communicate with one another to reach a consensus and synchronize prior to performing DBF. These inter-node communications may be hampered if the N active nodes are scattered throughout the larger area of $D(O, R_o)$.

3.3. The network connectivity: The following theorem from [6] is fundamental for our argument on the network connectivity.

Theorem 2: Consider a randomly selected point F on the ring $S(O, R_i, R_o)$ with a fix area of $A_S = \pi R_o^2 - \pi R_i^2$. Then, as R_o grows, the probability that another randomly selected point on $S(O, R_i, R_o)$ is in the R_f-neighborhood of F is given by $P_S = (\pi+1)R_f/2\pi R_o$. Now, consider a randomly selected point F on the disk $D(O, R_o)$. Then, as R_o grows, the probability that another randomly selected point on $D(O, R_o)$ is in the R_f-neighborhood of F is given by $P_D = R_f^2/R_o^2$.

Theorem 2 shows that, if the nodes transmission range is R_f, then, for a large R_o, the probability that two arbitrary active nodes are within the transmission range of each other is inverse proportional to R_o when the nodes are selected from $S(O, R_i, R_o)$ and inverse proportional to R_o^2 when they are selected from $D(O, R_o)$. Therefore, when both $S(O, R_i, R_o)$ and $D(O, R_o)$ have the same number of active nodes, the probability that some nodes in $D(O, R_o)$ lose contact with other active nodes is much higher. In such a case, the only approach to maintain the inter-node communications is to activate some of the sleeping nodes and use them as intermediate relays. This multi-hop scheme, in turns, may result in delay, degrading the synchronization accuracy, and the waste of transmission power.

3.4. Approximate average beampattern: It is usually desired to have a narrow mainlobe, or, equivalently, have $\phi_{(n),1}$ close to zero. According to the discussion in Subsection 3.1., $\phi_{(n),1}$ can be considered inverse proportional to R_o. Therefore, a small $\phi_{(n),1}$ requires a large R_o. At the same time, due to our discussions about the network energy preservation and the network connectivity in Subsections 3.2. and 3.3., it may be preferable to keep $A_S = \pi R_o^2 - \pi R_i^2$ just large enough to make sure that $S(O, R_i, R_o)$ includes N nodes. It is direct to observe that increasing R_o while keeping A_S fixed, results in an R_i that is very close to R_o, or, equivalently, a
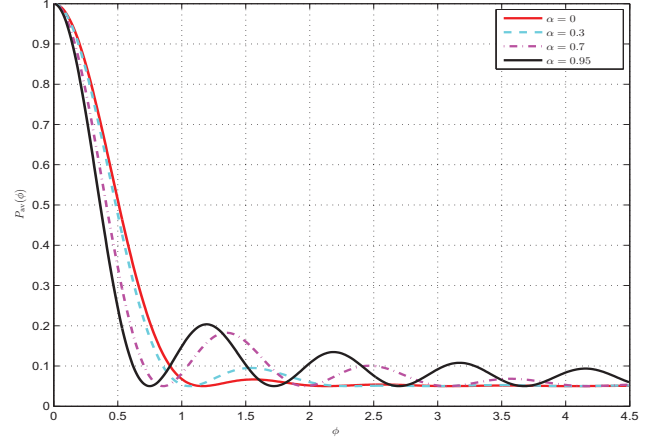

Fig. 1. $P_{\mathrm{av}}(\phi)$ versus ϕ for $R_o/\lambda = 10$ and different α.

large but narrow ring $S(O, R_i, R_o)$. It can be shown [6] for such a scenario that $P_{\mathrm{av}}(\phi)$ in (6) simplifies to

$$P_{\mathrm{av}}(\phi) \approx \frac{1}{K} + \left(1 - \frac{1}{K}\right)|J_0(R_o\beta(\phi))|^2. \qquad (8)$$

When $R_o\beta(\phi) \gg 1/4$, $P_{\mathrm{av}}(\phi)$ can be further simplified to

$$P_{\mathrm{av}}(\phi) \approx \frac{1}{K} + \left(1 - \frac{1}{K}\right)\frac{2}{\pi R_o\beta(\phi)}\cos^2\left(R_o\beta(\phi) - \frac{\pi}{4}\right). \quad (9)$$

Let $\phi_{(n),l}$ and $\phi_{(p),l}$ denote the l-th null and the l-th peak points of the average beampattern $P_{\mathrm{av}}(\phi)$, respectively (note that $\phi_{(p),0} = \phi_0 = 0$). From (9), it directly follows that

$$\phi_{(n),l} \approx 2 \arcsin\left(\frac{\lambda(l-1/4)}{4R_o}\right), \quad \phi_{(p),l} \approx 2 \arcsin\left(\frac{\lambda(l+1/4)}{4R_o}\right) \tag{10}$$

for $l = 1, 2, \ldots$. It follows from (9) and (10) that the l-th local maxima of the average sidelobe is approximately given by

$$P_{\mathrm{av}}(\phi_{(p),l}) \approx \frac{1}{K} + \left(1 - \frac{1}{K}\right)\frac{2}{\pi^2(l+1/4)}. \qquad (11)$$

Note that, $P_{\mathrm{av}}(\phi_{(p),l})$ is inverse proportional to l for large K. It should also be mentioned that the approximation obtained from (10) for $\phi_{(n),1}$ is in fact very close to $\phi_{(n),1} = 2 \arcsin\left((4\pi R_o)^{-1}\lambda\nu_0\right)$ derived in Subsection 3.1.

Note that, Equations in (10) provide a very simple technique to determine R_o and R_i: Given a desired $\phi_{(n),l}$ or $\phi_{(p),l}$, one may determine the required R_o from (10), and, then, use the preassigned $A_S = \pi R_o^2 - \pi R_i^2$ to derive R_i.

Fig. 1 shows $P_{\mathrm{av}}(\phi)$ versus ϕ for $K = 20$, $R_o/\lambda = 10$, and four different values of α. As expected, increasing α narrows down the mainlobe. Note also that, the area that includes the active nodes when $\alpha = 0$ is over 100 times more than the area that includes the active nodes when $\alpha = 0.95$. This facilitates leaving most of the nodes in the sleeping mode in the latter case and save substantial amount of energy. Note also that the larger values of α result in increased sidelobe peak levels. In Section 4, a simple technique is introduced to alleviate this problem.

3.5. Average directivity: Average directivity $D_{\mathrm{av}} \triangleq \mathrm{E}\{\int_{-\pi}^{\pi} P(0, \mathbf{z})d\phi / \int_{-\pi}^{\pi} P(\phi, \mathbf{z})d\phi\}$ is a parameter that

measures the efficiency of the beamforming technique to direct the transmitted power towards the desired direction. The so-defined D_{av} cannot be calculated in a closed form for the proposed algorithm. However, it is known that [1] D_{av} always lower-bounded by $\tilde{D}_{av} = 2\pi/\int_{-\pi}^{\pi} P_{av}(\phi)d\phi$. For the case that (8) holds, it is shown in [6] that $\tilde{D}_{av}/K = (1+(K-1)\,{}_2F_3(\frac{1}{2},\frac{1}{2};1,1,1,-(4\pi R_o/\lambda)^2))^{-1}$ where ${}_2F_3(\frac{1}{2},\frac{1}{2};1,1,1,-(4\pi R_o/\lambda)^2)$ is a generalized hypergeometric function. Moreover, it holds for large R_o/λ that [6] $D_{av}/K \geq \left(1+\mu(K-1)\frac{\ln(R_o/\lambda)}{(R_o/\lambda)}\right)^{-1}$ with $\mu \approx 0.0322$. It can be observed from the latter inequality that, as R_o increases, D_{av} reaches its maximum possible value of K.

4. MULTI-RING EXTENSION OF THE ALGORITHM

It follows from (11) that, when $R_i \approx R_o$, the first and the largest sidelobe peak of the average beampattern is given by $P_{av}(\phi_{(p),l}) \approx 0.16 + 0.84/K$ which is more than 16% of the mainlobe maxima. In applications that such a level of sidelobe peak is not acceptable, the nodes may be selected from multiple concentric rings of proper radii to decrease the sidelobe peak level. To substantiate this claim, let us assume that the K nodes used in the DBF are randomly selected from M concentric rings of $S_m(O, R_{m,i}, R_{m,o})$, $m = 1, \ldots, M$ where $R_{m,o} \leq R_{m+1,i}$. It can be shown that $P_{av}(\phi)$ is given by (6) where

$$\mathrm{E}\left\{e^{j\beta(\phi)Z}\right\} = \frac{2\sum_{m=1}^{M} R_{m,o}J_1\left(R_{m,o}\beta(\phi)\right) - R_{m,i}J_1\left(R_{m,i}\beta(\phi)\right)}{\beta(\phi)\sum_{m=1}^{M} R_{m,o}^2 - R_{m,i}^2}. \tag{12}$$

Assume that $A_{S_m} = \gamma/M$ for $m = 1, \ldots, M$, that is, all the concentric rings have the same area and their total area is equal to γ. Note that γ is independent from $R_{m,o}$ and if $R_{m,o}$ grows, $R_{m,i}$ increases as well such that $\gamma/M = \pi(R_{m,o}^2 - R_{m,i}^2)$ remains unchanged. Under the above condition, $P_{av}(\phi)$ simplifies for large $R_{1,o}$ to [6]

$$P_{av}(\phi) \approx \frac{1}{K} + \left(1 - \frac{1}{K}\right)\left|\frac{\sqrt{2}}{M}\sum_{m=1}^{M}\frac{\cos\left(R_{m,o}\beta(\phi) - \frac{\pi}{4}\right)}{\sqrt{\pi R_{m,o}\beta(\phi)}}\right|^2. \tag{13}$$

It can be observed from the above approximation that the contributions of all rings to $P_{av}(\phi)$ are simply summed up inside the absolute value at the right-hand side (RHS) of (13). This fact facilitates a simple technique to determine $R_{m,o}$, $m = 1, \ldots, M$ as follows. Assume that it is required to have a null at ϕ^*. Selecting

$$R_{m,o} = \frac{\lambda(m - 1/4)}{4\sin(\phi^*/2)}, \qquad m = 1, \ldots, M \tag{14}$$

all the cosine functions at the RHS of (13) are equal to zero at $\phi = \phi^*$, while each of these functions has its first maxima at a different point. This results in generating an average beampattern null at ϕ^* while substantially reducing the sidelobe peaks.

Fig. 2 shows $P_{av}(\phi)$ versus ϕ for $\lambda = 3$ m, $K = 20$, $\gamma = 25\pi$ m², $\phi^* = \pi/180$, and for the cases of $M = 1$, $M = 2$, and $M = 3$. $R_{m,o}$ is obtained from (14), while $R_{m,i}$ is calculated from $\gamma/M = \pi(R_{m,o}^2 - R_{m,i}^2)$. As can be observed from the figure, even two concentric rings considerably decrease the sidelobe peaks, and, at the same time, flatten the average beampattern around the null point $\phi^* = \pi/180$.
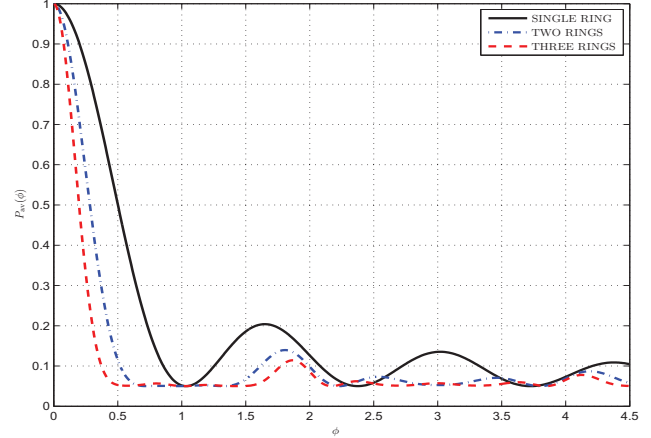

Fig. 2. $P_{av}(\phi)$ versus ϕ for $M = 1$, $M = 2$, and $M = 3$.

5. CONCLUSIONS

In this paper, a simple beamforming technique has been proposed for uniformly distributed wireless sensor networks. It has been shown that if the participating nodes in the beamforming are randomly selected from a narrow ring, an average beampattern with a narrow mainlobe can be generated, and, at the same time, a substantial amount of network energy may be preserved, and, further, the probability that the active nodes fall outside of the transmission range of one another is reduced. Then, an extension of the proposed technique has been presented and it has been shown that the sidelobe peaks can be considerably decreased if the nodes are selected from a few concentric rings.

6. REFERENCES

[1] H. Ochiai, P. Mitran, H. V. Poor, and V. Tarokh, "Collaborative beamforming for distributed wireless ad hoc sensor networks," *IEEE Trans. Signal Process.*, vol. 53, pp. 4110-4124, Nov. 2005.

[2] R. Mudumbai, G. Barriac, U. Madhow, "On the feasibilty of distributed beamforming in wireless sensor networks," *IEEE Trans. Wirless Commun.*, vo. 6, pp. 1754-1763, May 2007.

[3] M. F. A. Ahmed and S. A. Vorobyov, "Collaborative beamforming for wireless sensor networks with Gaussian distributed sensor nodes," *IEEE Trans. Wireless Commun.*, to appear.

[4] S. Boyd, A. Ghosh, B. Prabhakar, and D. Shah, "Randomized gossip algorithms," *IEEE Trans. Inf. Theory*, vo. 52, pp. 2508-2530, June 2006.

[5] D. R. Brown III and H. V. Poor, "Time-slotted round-trip carrier synchronization for distributed beamforming," *IEEE Trans. Signal Process.*, to appear.

[6] K. Zarifi, A. Ghrayeb, and S. Afess, "Collaborative beamforming for uniformly distributed wireless sensor networks," *IEEE Trans. Signal Process.*, submitted.

[7] W. Ye, J. Heidemann, and D. Estrin, "Medium access control with coordinated adaptive sleeping for wireless sensor networks," *IEEE/ACM Trans. Networking*, vol. 12, pp. 493-506, June 2004.